



## Bioinspired stimuli-responsive spindle-knotted fibers for droplet manipulation

Chaoyu Yang<sup>a,b,c</sup>, Yunru Yu<sup>a,c</sup>, Xiaocheng Wang<sup>c</sup>, Yan Zu<sup>c,\*</sup>, Yuanjin Zhao<sup>a,c,\*</sup>, Luoran Shang<sup>a,b,\*</sup>

<sup>a</sup> Department of Clinical Laboratory, Nanjing Drum Tower Hospital, School of Biological Science and Medical Engineering, Southeast University, Nanjing 210096, China

<sup>b</sup> Shanghai Xuhui Central Hospital, Zhongshan-Xuhui Hospital, and the Shanghai Key Laboratory of Medical Epigenetics, the International Co-laboratory of Medical Epigenetics and Metabolism (Ministry of Science and Technology) Institutes of Biomedical Sciences, Fudan University, Shanghai 200032, China

<sup>c</sup> Oujiang Laboratory (Zhejiang Lab for Regenerative Medicine, Vision and Brain Health), Wenzhou Institute, University of Chinese Academy of Sciences, Wenzhou 325001, China



### ARTICLE INFO

#### Keywords:

Bio-inspired  
Spindle-knot  
Stimuli-responsive  
Microfiber  
Droplet manipulation

### ABSTRACT

Manipulation of small amounts of liquids is of great importance in bio/chemical analysis, environmental engineering, medical diagnostics, etc. Novel platforms with systematic maneuverability and expanded applications are highly desired. Here, inspired by the directional liquid motion ability of natural fibrous materials, we present light-responsive spindle-knotted microfibers from piezoelectric microfluidics for droplet manipulation. The graphene oxide (GO) and poly(*N*-isopropylacrylamide) [poly(NIPAM)] components endow the fiber with near-infrared (NIR) stimuli-responsiveness. Besides, its unique structure enables droplet pinning in the knots of the fiber. During NIR irradiation, the fiber can shrink and turn hydrophobic, which resulted in directional droplet migration from one knot to another. Based on this phenomenon, controllable droplet merging could be initiated under light control, and chemical reactions could be carried out on-site. More intriguingly, systematic manipulation of droplet pathways was achieved through a woven fiber network, by which multi-step reactions could occur orderly. These features indicated that the bio-inspired photo-controllable spindle-knotted fibers would find vast opportunities in broad applications, such as micro-reactors and optofluidic systems.

### 1. Introduction

Manipulating small volumes of liquids is critical in both scientific sense and practical applications including biological and/or chemical reactions, medical diagnostics, environmental engineering, etc [1–5]. Currently, a diversity of paradigms have been developed to control liquid droplets with the assistance of micro-/nano-structured interfaces or external forces such as electric/magnetic fields [5–9], mechanical vibration [4,10,11], light [12–15], etc. With these efforts, functional liquid manipulation systems have been constructed and demonstrated potential values in various fields, including fog harvest [16], directional liquid transport [17], oil/water separation [18], anti-icing/fogging [19], microfluidics[14], etc. Although with these remarkable achievements, the demanding requirements for liquid control in practical applications still call for the creation of advanced manipulation approaches. Thus, novel feasible and easy-to-operate liquid control

platforms with systematic maneuverability and expanded applications are still worth seeking.

Here, inspired by the directional liquid transport phenomenon of spider silks and the underlying mechanisms regarding a heterogeneously textured bump structure, we present microfluidic-derived stimuli-responsive spindle-knotted fibers for droplet manipulation, as shown in Fig. 1. Microfibers with specific topographies and microstructures play indispensable roles in biological activities and attract extensive attention as synthetic materials for their broad implications [20–22]. Inspired by the highly-specialized spinning process in living organisms, various methods have been developed to construct artificial microfibers, such as direct writing, wet/dry spinning, electrospinning, and microfluidics [23–29]. Particularly, microfluidics is known for the precise control of small volumes of fluids and multiphase flow interfaces within constrained channels [30–36]. Taking advantage of this, microfluidics has been well implemented in the consecutive generation of

\* Corresponding authors at: Department of Clinical Laboratory, Nanjing Drum Tower Hospital, School of Biological Science and Medical Engineering, Southeast University, Nanjing 210096, China (Y. Zhao and L. Shang).

E-mail addresses: [zuyan@foxmail.com](mailto:zuyan@foxmail.com) (Y. Zu), [yjzhao@seu.edu.cn](mailto:yjzhao@seu.edu.cn) (Y. Zhao), [luoranshang@fudan.edu.cn](mailto:luoranshang@fudan.edu.cn) (L. Shang).

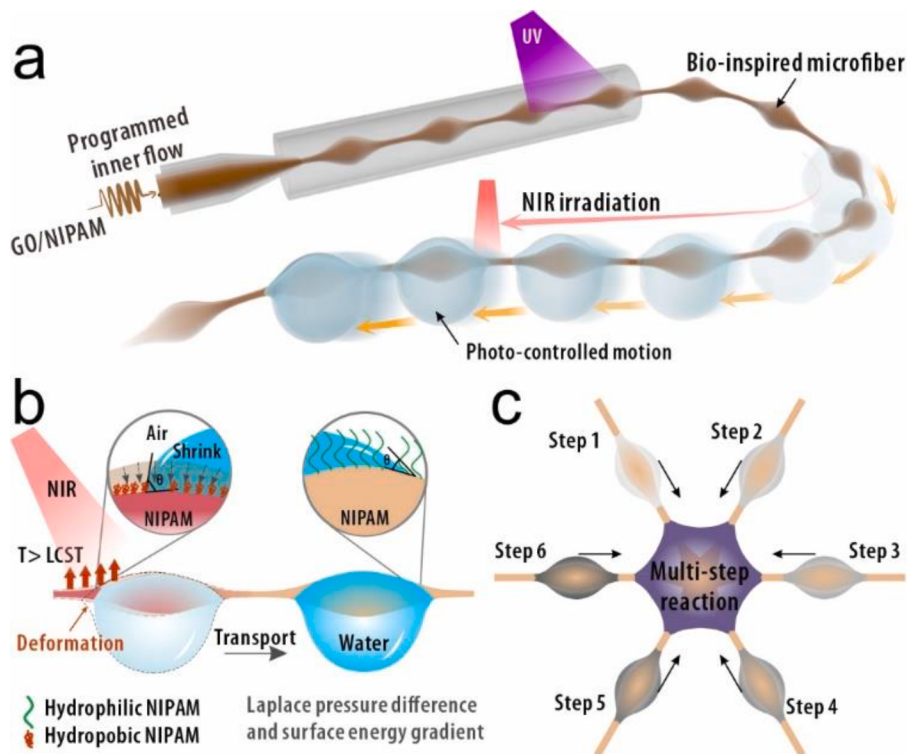


**Fig. 1.** Schematic illustrations of (a) piezoelectric microfluidic generation of bioinspired stimuli-responsive spindle-knotted fibers and the NIR-controlled droplet directional movement; (b) mechanism of the photothermally responsive water-transportation behavior; (c) a multi-step reaction taken place in a woven network of the stimuli-responsive fibers.

microfibers with straight, helical, Janus, multicompartmental, and spindle-knot morphologies [37–43]. Although these microfibers have been applied in water collection, their capability of active water transportation remains less explored.

Herein, we constructed a fiber-based liquid transport platform via piezoelectric-assisted microfluidic spinning. By introducing programmed vibrations to a microfluidic jet flow and polymerizing the jet *in-situ* through ultraviolet (UV) irradiation, fibers composed of poly (NIPAM) and graphene oxide (GO) with periodic knot structures were continuously generated. Taking advantage of the excellent photo-thermal transformation of GO and the temperature-induced phase transition of poly(NIPAM), the obtained hydrogel fibers could behave near-infrared (NIR)-reactiveness volume change. As a result, a Laplace pressure difference and wettability gradient were established along the fiber, which can propel droplets moving away from the light source. With this feature, fundamental operations including directional droplet moving and merging were readily achieved. It is worth mentioning that the systematic manipulation of droplet paths was accomplished based on woven fiber networks with complex spatial configurations, by which multistep reactions could be executed with a single beam of light. These results indicated that the bioinspired stimuli-responsive spindle-knotted fibers have great potential in liquid manipulation and the relevant application fields.

## 2. Experimental section

### 2.1. Materials:

PEG-diacylate (PEGDA, average Mn = 700), and *N,N'*-methylenebis(acrylamide) (BIS) were brought from Sigma Aldrich. Sodium alginate (SA), Calcium chloride (CaCl<sub>2</sub>), Sodium hydroxide (NaOH), Hydrochloric acid (HCl), and Copper sulfate (CuSO<sub>4</sub>) were purchased from Sinopharm Chemical Reagent Co., Ltd. Fluorescent polystyrene nanoparticles (F8811) was procured from Invitrogen. The concentration of

graphene oxide (GO, XF NANO) solution was 2 mg/mL. *N*-Isopropylacrylamide (NIPAM, 97 %) was from Macklin. The photo-initiator was Lithium phenyl(2,4,6-trimethylbenzoyl) phosphinate (LAP, Aladdin).

## 2.2. Experiments

### 2.2.1. Piezoelectric microfluidics construction

The inner cylindrical capillary with an inner diameter (ID = 580 μm) and outer diameter (OD = 1 mm) was tapered and sanded to the desired diameter (about 200 μm). Then another capillary (ID = 1.56 mm, OD = 2 mm) was coaxially nested outside of the previous one. The joints of these capillaries were sealed by transparent epoxy resin. To generate wavy jet templates, we employed a piezoelectric stack to transmit the sinusoidal vibration to the inner phase. The piezoelectric stack actuator was connected to a signal generator (Siglent, SDG 2000X) via a power amplifier (Core morrow, E-05) to program the amplitudes and frequencies, as shown in Figure S1. In this paper, the magnification of the power amplifier was fixed as 12×, and the voltages mentioned throughout the manuscript were in the form of V<sub>p-p</sub> (peak-to-peak) of the signal generator.

### 2.2.2. Bioinspired stimuli-responsive spindle-knotted microfibers generation

For the generation of knot microfibers, the inner phase was a mixture solution of GO (1.6 mg/mL), NIPAM (6.4 % v/v), PEGDA (4 % v/v), BIS (corresponding to 1/30 to the mass of NIPAM), SA (0.4 % v/v), and LAP (0.1 % v/v); the outer flow was deionized water. The representative inner and outer flow rates were 5 mL/h and 30 mL/h, respectively. Both solutions were driven into the corresponding channels by two syringe pumps (Longer, LSP01-2A) and the inner phase was connected to the piezoelectric stack actuator. Green fluorescent polystyrene (PS) nanoparticles were added to the inner phase at a concentration of 0.5 % v/v for fluorescent imaging. Finally, the wavy jet templates were rapidly solidified downstream upon *in-situ* ultraviolet (UV) irradiation (EXFO

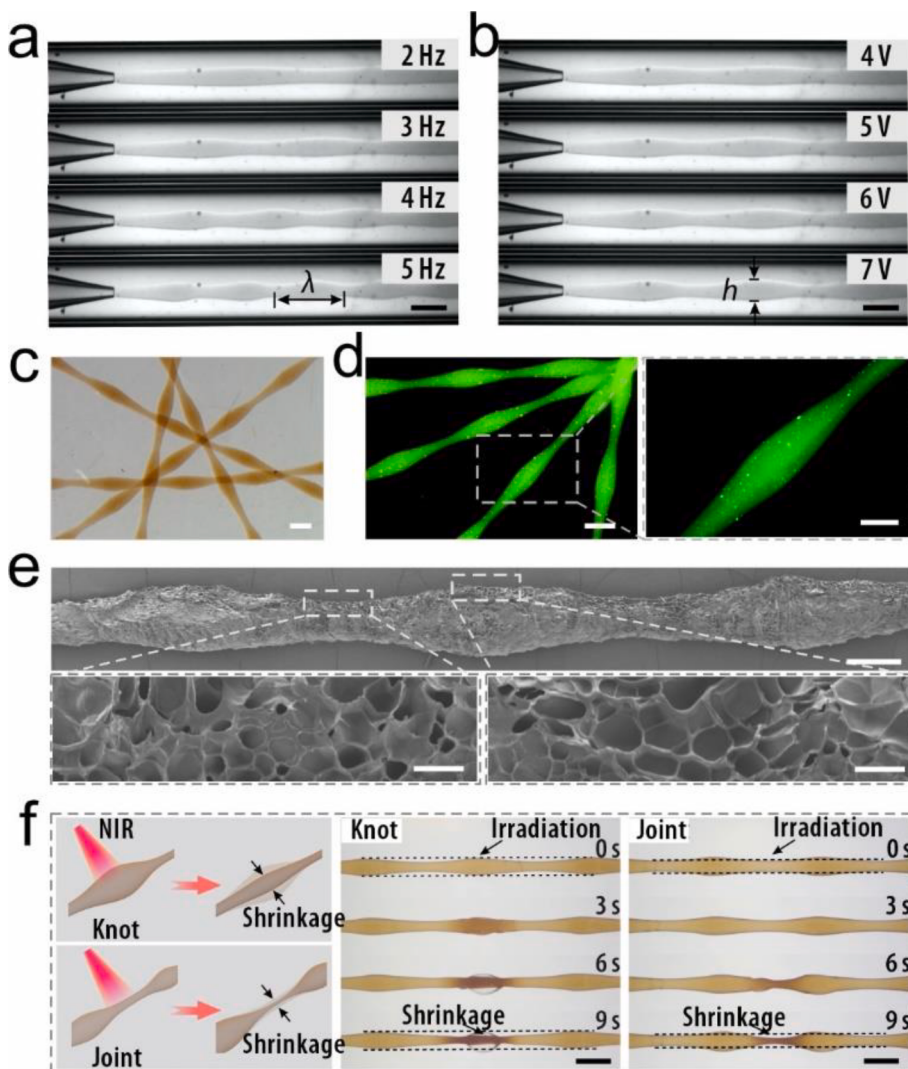


**Fig. 2.** (a, b) Real-time images of the wavy jet template fabrication under different (a) piezoelectric frequencies and (b) amplitudes. The flow rates were  $Q_i = 5 \text{ mL/h}$ , and  $Q_o = 30 \text{ mL/h}$ , respectively; (c) microscopic image of the spindle-knotted fibers; (d) fluorescent images of the spindle-knotted fibers. The right image is an enlarged view showing the compositional homogeneity; (e) SEM images of the fiber after freeze-drying and detailed views of the knots and joints; (f) schemes and images of the responsive behavior of the fibers with NIR irradiation pointed at the knot and joint. The scale bars are 1000  $\mu\text{m}$  in (a, b, c, left panel of d, and f), 500  $\mu\text{m}$  in the right panel of (d), 500  $\mu\text{m}$  in the top panel of (e), and 50  $\mu\text{m}$  in the bottom panel of (e).

OmniCure SERIES 1000, 365 nm, 100 W). The resultant fibers were collected in  $\text{CaCl}_2$  solution (2 wt%) to facilitate cross-linking of sodium alginate and then washed 5 times for removing the residual  $\text{CaCl}_2$  from fiber surfaces.

#### 2.2.3. Characterization

The microfluidic spinning of piezoelectric-actuated wavy jet was observed by a microscope (OLYMPUS, CKX53) and a high-speed camera (AcutEye). Microscopic images of the resultant microfibers were captured by a fluorescent microscope (OLYMPUS, SZX16). The microstructures of resultant microfibers were from scanning electron microscopy (SEM, HITACHI, SU8010). The droplet transport processes were recorded by the same high-speed camera with a horizontal lens (front view) and a CCD on stereomicroscope (top view). The water contact angles ( $5 \mu\text{L}$ ) were measured by using a contact angle measuring system (JC2000D2). The NIR stimuli were carried out via a NIR system (808 nm) with a power of  $10 \text{ W/cm}^2$  and distance of about 1 cm.

### 3. Results and discussion

In a typical experiment, the inner phase of a GO/NIPAM pre-gel solution was driven through the tapered injection capillary, and the outer aqueous phase was driven in the same direction into the collection capillary of the microfluidic device. Upon piezoelectric vibration, a programmed wavy jet was formed downstream at the same frequency as

the vibration in the collection tube due to the ultralow surface tension of the aqueous-aqueous fluids system, as shown in Figure S2, S3, and Movie S1. During this process, the jet configuration could be easily tuned because of the diverse sets of flow rates and piezoelectric parameters. In specific, the wavelength  $\lambda$  and the height  $h$  of the wave showed relationships with the piezoelectric frequency and the maximum voltage amplitude (Fig. 2a, 2b, Figure S4 and Note S1). After *in situ* solidification by UV irradiation, spindle-knot microfibers were collected at the outlet of the microfluidic device, as shown in Fig. 2c and Figure S5. Since the formation of knots and joints resulted from the pulsation of a single jet, the fibers exhibited homogeneous composition along, as confirmed in the fluorescence and Scanning Electron Microscope (SEM) images (Fig. 2d, 2e).

Graphene oxide (GO) is regarded as a typical two-dimensional carbon material with excellent photothermal conversion ability. Meanwhile, poly(NIPAM) is a thermal-responsive polymer, which would shrink and become hydrophobic when the surrounding temperature exceeds its phase inversion temperature. The integration of these two compositions would impart the fibers with excellent NIR stimuli-responsive capacity. As such, the behavior of GO/poly(NIPAM) fibers under NIR irradiation was firstly investigated. It was found that the GO/poly(NIPAM) composite fiber (including knots and joints) shrank due to photothermally triggered deswelling (Fig. 2f). It was worth mentioning that the compositional homogeneity of the fiber ensured that the knots and joints had the same stimuli-responsive features (Figure S6), thereby

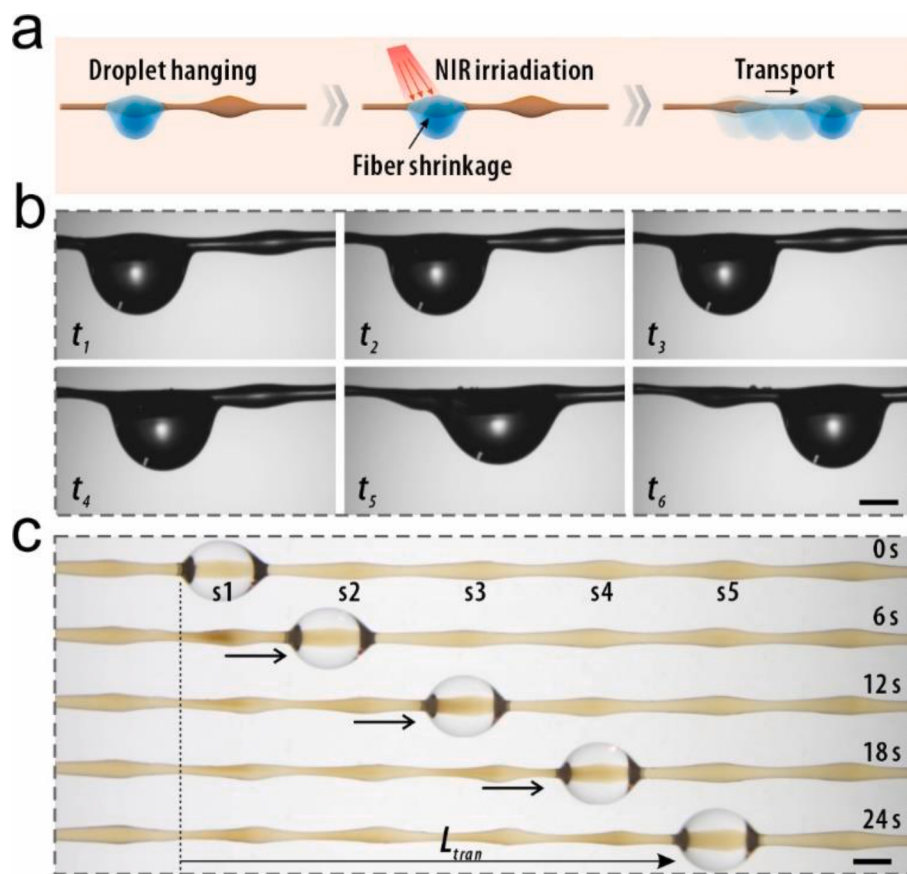


**Fig. 3.** (a) Schematic of droplet transportation between the knots on the bio-inspired microfiber under irradiation stimuli; (b) microscopic images of a water droplet ( $4 \mu\text{L}$ ) transporting to the neighboring knot; (c) long-distance transport of a single droplet ( $4 \mu\text{L}$ ) along the microfiber. The scale bars are  $1000 \mu\text{m}$ .

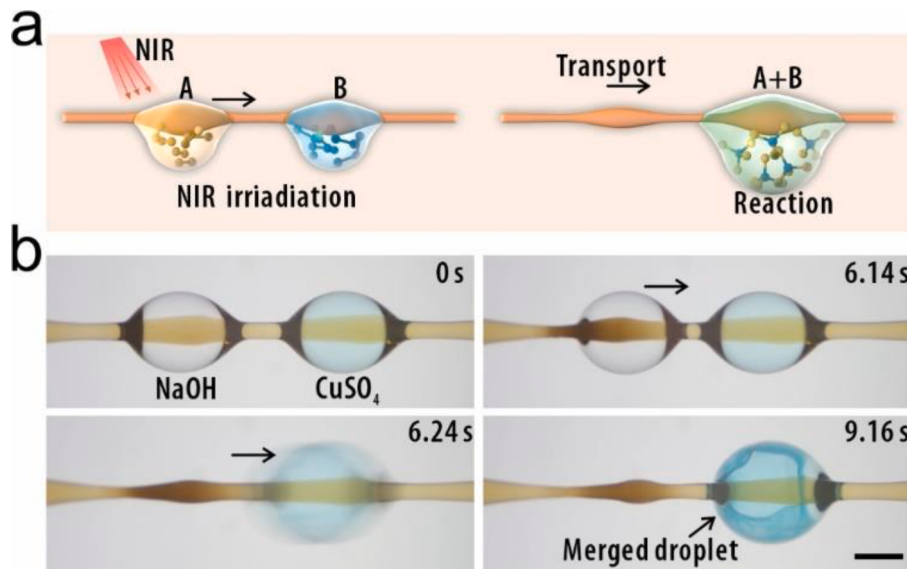


**Fig. 4.** (a) Schematic of the functional microfiber accommodating droplet reaction; (b) time-sequential images showing the synthesis of  $\text{Cu}(\text{OH})_2$  based on the droplet ( $4 \mu\text{L}$ ) microreactors. The scale bar is  $1000 \mu\text{m}$ .

endowing the potential to transport droplets in long-distance (from knot to knot).

Benefiting from the excellent photothermal responsive behaviors, we explored the liquid transport capability of the GO/poly(NIPAM) composite fiber, as illustrated in Fig. 3a. A microfiber was placed horizontally and a droplet ( $4 \mu\text{L}$ ) was suspended over a knot by a pipette.

Because of the excellent water adhesion ability of the knot, a droplet could be easily pinned at the knot position (Figure S7). It was found that the fiber significantly shrank at the NIR irradiating position, even with the presence of a droplet. This not only increased the curvature of the knot but also significantly changed the surface wettability (Figure S8). As a result, the droplet would be driven away from the NIR light source

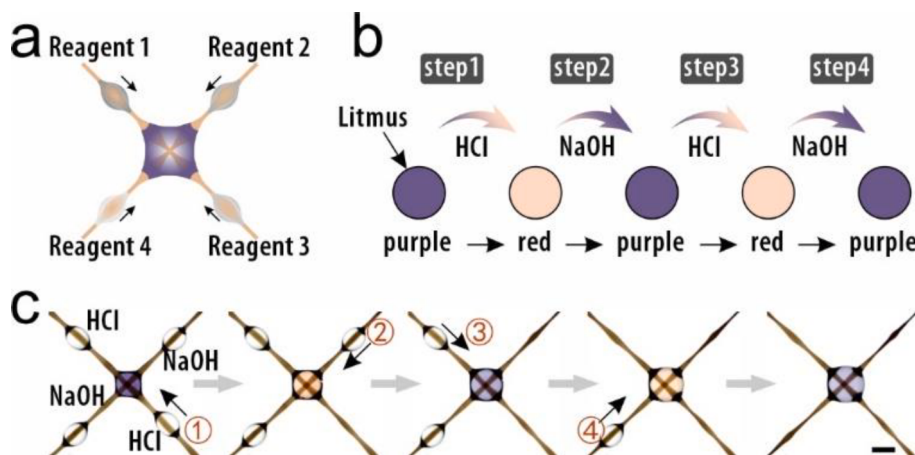


**Fig. 5.** (a) Schematic figure of a convergent fiber network for multi-reagent reaction; (b) the designed multi-step reaction process; (c) sequential images of the multi-step reactions of converging droplets in the fiber network. The scale bar is 2 mm.

and transported from the initial knot along the joint, eventually hanging on the adjacent knot because of the concurrent surface energy gradient and Laplace pressure difference (Fig. 1b and Note S2). The transport process was recorded by a high-speed camera, as shown in Fig. 3b, Figure S9, and Movie S2. Based on this operation, controllable long-distance water transport along the GO/poly(NIPAM) composite spindle-knot microfiber could be realized by repeating the NIR guiding process. To test this, a long fiber with multiple knots was constructed with a water droplet hanging on a knot (Fig. 3c, Movie S3). With continuous irradiation, the droplets were successfully transferred from the initial knot s1 to knot s5 under remote control, traveling a distance of  $L_{\text{trans}} \approx 11.18$  mm in 24 s. These results showed that the microfiber was conceivably able to realize light-stimulated droplet transport.

The light-controlled active transport of water droplets on the fibers can be harnessed for many practical applications. For instance, we performed droplet merging using a single beam of NIR. We further demonstrated that the droplets could be utilized as microreactors for chemical reactions (Fig. 4a). As a proof-of-concept, a pair of droplets containing NaOH and CuSO<sub>4</sub> aqueous solution, respectively, was propelled to coalesce under NIR stimulation, with blue precipitates immediately formed in the merged droplet, suggesting the synthesis of Cu(OH)<sub>2</sub> (Fig. 4b). The reaction would be accelerated to a certain degree because the vibration resulted from the droplet collision would improve the mixing of reagents. Notably, when the total volume of the two droplets exceeded the hanging capacity of the knot, the droplets fell off spontaneously (Figure S10), which would benefit the collection of the reaction product. These results indicated that the bioinspired microfibers are reliable containers suitable for chemical reactions.

Based on the droplet manipulation ability of the bio-inspired stimuli-responsive microfibers, we designed a fiber network with a convergent configuration for multi-droplet merge. As shown in Fig. 5a, by arranging the microfibers in a radial shape, water droplets in the knot of the fiber branch could aggregate towards the intersection following a preset order and merge to form a huge droplet (Figure S11). With this, we carried out a multi-step acid-base reaction indicated by alternating color changes. As shown in Fig. 5b, a four-branch fiber network was built with one droplet of litmus hung in the intersection and two droplets of hydrochloric acid as well as another two droplets of sodium hydroxide placed in the knot of each branch. Then, the four droplets moved to the intersection in sequence in the order of the NIR irradiation and eventually coalesced with the droplet in the center. During the sequential merging process, the color of the center droplet turned red and purple alternately (Fig. 5c). These results further validated the value of the stimuli-responsive fibers as microreactors and suggested their potential for undertaking complex chemical reactions.

#### 4. Conclusion

In summary, we presented bio-inspired light-responsive spindle-knotted microfibers with compositional homogeneity via a piezoelectric microfluidic spinning approach. Benefiting from the photothermal responsiveness of the GO/poly(NIPAM) composite, the resultant microfibers could shrink and turn hydrophobic at the place under NIR irradiation. The resultant Laplace pressure difference and surface energy gradient could drive liquid movement away from the light source. This mechanism, combined with the unique knot structure of the fiber that enabled the pinning of droplets, provided a novel light-stimulated droplet manipulation platform. Based on this, a microreaction system was established with hanging drops serving as reactors and their coalescence behaviors, guided by NIR, initiated the reactions on site. Moreover, a pre-woven fiber network was built to carry out multi-step reactions following a preset sequence. The potential applications of this strategy can be expanded by developing alternative stimuli-responsive materials (e.g. liquid crystal) and designing more complex network topologies. These results indicated that the bioinspired stimuli-responsive spindle-knotted fibers provide a facile and intelligent way of droplet manipulation and would shed light on multidisciplinary application areas.

#### Declaration of Competing Interest

The authors declare that they have no known competing financial interests or personal relationships that could have appeared to influence the work reported in this paper.

#### Data availability

Data will be made available on request.

#### Acknowledgements

This work was supported by the National Key Research and Development Program of China (2020YFB1313100), the National Natural Science Foundation of China (22002018), the Guangdong Basic and Applied Basic Research Foundation (2021B1515120054), and the Shenzhen Fundamental Research Program (JCYJ20190813152616459 and JCYJ20210324133214038), and the China Postdoctoral Science Foundation (2022M713103).

#### Author contributions

Y. Z. conceived the idea and designed the experiment; C. Y. carried

out the experiments and analyzed data; C. Y. and L. S. wrote the paper; Y. Y. and X. W. contributed to the scientific discussion of the article.

## Appendix A. Supplementary data

Supplementary data to this article can be found online at <https://doi.org/10.1016/j.cej.2022.138669>.

## References

- [1] X. Liu, N. Kent, A. Ceballos, R. Streubel, Y. Jiang, Y. Chai, P.Y. Kim, J. Forth, F. Hellman, S. Shi, Reconfigurable ferromagnetic liquid droplets, *Science* 365 (6450) (2019) 264–267.
- [2] W. Li, X. Tang, L. Wang, Photopyroelectric microfluidics, *Sci. Adv.* 6 (38) (2020) eabc1693.
- [3] Q. Sun, D. Wang, Y. Li, J. Zhang, S. Ye, J. Cui, L. Chen, Z. Wang, H.-J. Butt, D. Vollmer, Surface charge printing for programmed droplet transport, *Nat. Mater.* 18 (9) (2019) 936–941.
- [4] Y. Zhang, J. Li, L. Xiang, J. Wang, T. Wu, Y. Jiao, S. Jiang, C. Li, S. Fan, J. Zhang, A Biocompatible Vibration-Actuated Omni-Droplets Rectifier with Large Volume Range Fabricated by Femtosecond Laser, *Adv. Mater.* 34 (12) (2022) 2108567.
- [5] J. Hartmann, M.T. Schür, S. Hardt, Manipulation and control of droplets on surfaces in a homogeneous electric field, *Nat. Commun.* 13 (1) (2022) 1–10.
- [6] J. Wang, W. Gao, H. Zhang, M. Zou, Y. Chen, Y. Zhao, Programmable wettability on photocontrolled graphene film, *Sci. Adv.* 4 (9) (2018) eaat7392.
- [7] J. Li, N.S. Ha, T.L. Liu, R.M. van Dam, C.-j., C.J'Kim, Ionic-surfactant-mediated electro-dewetting for digital microfluidics, *Nature* 572 (7770) (2019) 507–510.
- [8] W. Wang, J.V. Timonen, A. Carlson, D.-M. Drotlef, C.T. Zhang, S. Kolle, A. Grinthal, T.-S. Wong, B. Hatton, S.H. Kang, Multifunctional ferrofluid-infused surfaces with reconfigurable multiscale topography, *Nature* 559 (7712) (2018) 77–82.
- [9] Y. Jin, W. Xu, H. Zhang, R. Li, J. Sun, S. Yang, M. Liu, H. Mao, Z. Wang, Electrostatic tweezer for droplet manipulation, *Proc. Natl. Acad. Sci. U. S. A.* 119 (2) (2022).
- [10] N.A. Malvadkar, M.J. Hancock, K. Sekeroglu, W.J. Dressick, M.C. Demirel, An engineered anisotropic nanofilm with unidirectional wetting properties, *Nat. Mater.* 9 (12) (2010) 1023–1028.
- [11] D. Wu, Z. Zhang, Y. Zhang, Y. Jiao, S. Jiang, H. Wu, C. Li, C. Zhang, J. Li, Y. Hu, High-Performance Unidirectional Manipulation of Microdroplets by Horizontal Vibration on Femtosecond Laser-Induced Slant Microwall Arrays, *Adv. Mater.* 32 (48) (2020) 2005039.
- [12] F. Wang, M. Liu, C. Liu, Q. Zhao, T. Wang, Z. Wang, X. Du, Light-induced charged slippery surfaces, *Sci. Adv.* 8 (27) (2022) eabp9369.
- [13] J. Wang, L. Sun, M. Zou, W. Gao, C. Liu, L. Shang, Z. Gu, Y. Zhao, Bioinspired shape-memory graphene film with tunable wettability, *Sci. Adv.* 3 (6) (2017) e1700004.
- [14] J.-A. Lv, Y. Liu, J. Wei, E. Chen, L. Qin, Y. Yu, Photocontrol of fluid slugs in liquid crystal polymer microactuators, *Nature* 537 (7619) (2016) 179–184.
- [15] D. Psaltis, S.R. Quake, C. Yang, Developing optofluidic technology through the fusion of microfluidics and optics, *Nature* 442 (7101) (2006) 381–386.
- [16] Y. Zheng, H. Bai, Z. Huang, X. Tian, F.-Q. Nie, Y. Zhao, J. Zhai, L. Jiang, Directional water collection on wetted spider silk, *Nature* 463 (7281) (2010) 640–643.
- [17] H. Dai, Z. Dong, L. Jiang, Directional liquid dynamics of interfaces with superwettability, *Sci. Adv.* 6 (37) (2020) eabb5528.
- [18] C. Li, L. Wu, C. Yu, Z. Dong, L. Jiang, Peristome-Mimetic Curved Surface for Spontaneous and Directional Separation of Micro Water-in-Oil Drops, *Angew. Chem.* 129 (44) (2017) 13811–13816.
- [19] J. Yong, Q. Yang, X. Hou, F. Chen, Nature-Inspired Superwettability Achieved by Femtosecond Lasers, *Ultrafast Science* 2022 (2022).
- [20] J. Yuan, W. Neri, C. Zakri, P. Merzeau, K. Kratz, A. Lendlein, P. Poulin, Shape memory nanocomposite fibers for untethered high-energy microengines, *Science* 365 (6449) (2019) 155–158.
- [21] X. Liao, M. Dulle, J.M.d.S. e Silva, R.B. Wehrspohn, S. Agarwal, S. Förster, H. Hou, P. Smith, A. Greiner, High strength in combination with high toughness in robust and sustainable polymeric materials, *Science* 366 (6471) (2019) 1376–1379.
- [22] X. Wang, C. Yang, Y. Yu, Y. Zhao, In Situ 3D Bioprinting Living Photosynthetic Scaffolds for Autotrophic Wound Healing, *Research* 2022 (2022).
- [23] L. Shang, Y. Yu, Y. Liu, Z. Chen, T. Kong, Y. Zhao, Spinning and Applications of Bioinspired Fiber Systems, *ACS Nano* 13 (3) (2019) 2749–2772.
- [24] C. Fu, Z. Shao, V. Fritz, Animal silks: their structures, properties and artificial production, *Chem. Commun.* 43 (2009) 6515–6529.
- [25] A. Stoddart, Spider silk: Spinning an artificial yarn, *Nat. Rev. Mater.* 2(2) (2017) 1–1.
- [26] Y.S. Zhang, A. Arneri, S. Bersini, S.-R. Shin, K. Zhu, Z. Goli-Malekabadi, J. Aleman, C. Colosi, F. Busignani, V. Dell'Erba, Bioprinting 3D microfibrous scaffolds for engineering endothelialized myocardium and heart-on-a-chip, *Biomaterials* 110 (2016) 45–59.
- [27] H. Chen, Y. Zhao, Y. Song, L. Jiang, One-step multicomponent encapsulation by compound-fluidic electrospray, *J. Am. Chem. Soc.* 130 (25) (2008) 7800–7801.
- [28] M. Zhang, S. Wang, Y. Zhu, Z. Zhu, T. Si, R.X. Xu, Programmable dynamic interfacial spinning of bioinspired microfibers with volumetric encoding, *Mater. Horiz.* 8 (6) (2021) 1756–1768.
- [29] J. Zhang, D. Sun, B. Zhang, Q. Sun, Y. Zhang, S. Liu, Y. Wang, C. Liu, J. Chen, J. Chen, Intrinsic carbon nanotube liquid crystalline elastomer photoactuators for high-definition biomechanics, *Mater. Horiz.* (2022).
- [30] A.K. Miri, D. Nieto, L. Iglesias, H. Goodarzi Hosseiniabadi, S. Maharjan, G.U. Ruiz-Esparza, P. Khoshakhlagh, A. Manbachi, M.R. Dokmeci, S. Chen, Microfluidics-enabled multimaterial maskless stereolithographic bioprinting, *Adv. Mater.* 30 (27) (2018) 1800242.
- [31] C. Yang, R. Qiao, K. Mu, Z. Zhu, R.X. Xu, T. Si, Manipulation of jet breakup length and droplet size in axisymmetric flow focusing upon actuation, *Phys. Fluids* 31 (9) (2019), 091702.
- [32] E. Kang, G.S. Jeong, Y.Y. Choi, K.H. Lee, A. Khademhosseini, S.H. Lee, Digitally tunable physicochemical coding of material composition and topography in continuous microfibres, *Nat. Mater.* 10 (11) (2011) 877–883.
- [33] Y. Yu, L. Shang, J. Guo, J. Wang, Y. Zhao, Design of capillary microfluidics for spinning cell-laden microfibers, *Nat. Protoc.* 13 (11) (2018) 2557–2579.
- [34] H.T. Liu, H. Wang, W.B. Wei, H. Liu, L. Jiang, J.H. Qin, A Microfluidic Strategy for Controllable Generation of Water-in-Water Droplets as Biocompatible Microcarriers, *Small* 14 (36) (2018) 1801095.
- [35] C. Yang, Y. Yu, X. Wang, Q. Wang, L. Shang, Cellular fluidic-based vascular networks for tissue engineering, *Eng. Regener.* 2 (2021) 171–174.
- [36] Y. Pan, Z. Yang, C. Li, S.U. Hassan, H.C. Shum, Plant-inspired TransOrigami microfluidics, *Science advances* 8 (18) (2022) eab01719.
- [37] Y. Cheng, F. Zheng, J. Lu, L. Shang, Z. Xie, Y. Zhao, Y. Chen, Z. Gu, Bioinspired Multicompartmental Microfibers from Microfluidics, *Adv. Mater.* 26 (30) (2014) 5184–5190.
- [38] J.K. Nunes, H. Constantin, H.A. Stone, Microfluidic tailoring of the two-dimensional morphology of crimped microfibers, *Soft Matter* 9 (16) (2013) 4227–4235.
- [39] Y. Yu, F. Fu, L. Shang, Y. Cheng, Z. Gu, Y. Zhao, Bioinspired Helical Microfibers from Microfluidics, *Adv. Mater.* 29 (18) (2017) 1605765.
- [40] J. Guo, Y. Yu, D. Zhang, H. Zhang, Y. Zhao, Morphological Hydrogel Microfibers with MXene Encapsulation for Electronic Skin, *Research* 2021 (2021).
- [41] C. Yang, Y. Yu, X. Wang, L. Shang, Y. Zhao, Programmable knot microfibers from piezoelectric microfluidics, *Small* 18 (5) (2022) 2104309.
- [42] J.H. Kim, K.H. Kim, G.H. Lee, J.-W. Kim, S.H. Han, C.-S. Lee, S.-H. Kim, Microfluidic Production of Mechanochromic Photonic Fibers Containing Nonclose-Packed Colloidal Arrays, *Small Science* 1 (4) (2021) 2000058.
- [43] Q. Ma, Y. Song, W. Sun, J. Cao, H. Yuan, X. Wang, Y. Sun, H.C. Shum, Cell-inspired all-aqueous microfluidics: from intracellular liquid–liquid phase separation toward advanced biomaterials, *Adv. Sci.* 7 (7) (2020) 1903359.